S. KULESZA*#, M. BRAMOWICZ*, M. GWOŹDZIK**, S.WILCZYŃSKI***,
A.M. GOŹDZIEJEWSKA*

STRUCTURAL AGING AND DEGRADATION OF HUMAN FINGERNAIL PLATES UPON COSMETIC AGENTS

The knowledge whether and how chemical species react with tissues is important because of protection against harmful factors, diagnose of dermatological diseases, validation of dermatological procedures as well as effectiveness of topical therapies. In presented work the effects of chemical agents on plates of human fingernails were studied using Atomic Force Microscopy and Scanning Electron Microscopy. Apart from that, mapping of the elastic properties of the nails was also carried out. To obtain reliable measures of spatial evolution of the surface variations, recorded images were analyzed in terms of scaling invariance brought by fractal geometry, instead of common though not unique statistical measures.

Keywords: Atomic Force Microscopy, Scanning Electron Microscopy, fractal characterization, nanoscale property mapping

1. Introduction

The problem of quantitative investigation of the nail plates at the micro- and nanoscale turns out to be of great importance for diagnosing a broad spectrum of dermatological diseases, validation of treatment procedures as well as analysis of effectiveness of topical medicines applied to the affected areas [1,2]. Development of procedures for qualitative characterization of fingernail plates may be relevant to determination of evolutionary mechanisms and post-exposure consequences of fungal and bacterial infections. For example, Liu et al. reported SEM observations of superfine structure of the nail plates suffered from chronic mucocutaneous candidiasis (CMC). Imaging revealed that the hyphae penetrated the nail plate from the ventral surface and started to build-in into it causing gradual degradation [3].

On the other hand, the assessment of a surface structure of the nail plates might be important for the treatment of other infections with various etiologies [4,5]. For example, surface energy of the fingernail plate is a factor that controls surface adhesion, and hence affects processes occurring on the plate: colonization by microorganisms and penetration by pathogens. Healthy nails exhibit surface energy around 34 mJ/m^2 [6], however, this energy can be substantially changed due to abrasion processes [6]. The abrasion also enhances surface development through creation of ridges and grooves while surface energy affects contact phenomena at the nail-liquid interface, which is of great importance for topical therapy of various nail diseases. Depending on the contact area, drug dissolution and bioavailability directly determine the effectiveness of the applied medicine [7].

Analysis of nails by means of AFM and SEM techniques prevails over other microscopic methods. First of all, the nails are made of hard tissues, which makes preparation of histopathological specimens tedious task [8]. To facilitate the thinning, various tissue softeners need to be used, for example: formalin [9], non-ionic surfactants (Tween) [10] or ethanol [11]. Unfortunately, the above compounds cause undesirable side effects upon application, substantially influencing biomechanical properties of the nail plates. Specimens for AFM imaging are not that restricted since the coupling medium contains water and cannot penetrate the nail plate. It should also be noted that in case of localized nail infections, pathogens may be found on the bottom side of the nail plate [12]. As a consequence, getting a swab culture will likely yield false-negative results. In spite of that, however, SEM images might reveal outbreaks of infection, even inactive, and help identify potential pathogen in order to optimize the treatment procedure [13,14].

Finally, spatial characterization of the structure of the nail plates is important from the point of view of effectiveness of the topical pharmacological treatment, which actually peaks at 15 percent at its best [13]. The main reason for that is low penetration rate of active substances through the nail plate, hence to increase the effectiveness of the topical therapy, various etching agents might be used including, among others: lactic acid, tartaric acid, glycolic acid, citric acid or 5-fluorouracil [13,15].

*   UNIVERSITY OF WARMIA AND MAZURY, 2 OPACZOWSKIEGO STR., 10-719 OLSZTYN, POLAND
**   CZESTOCHOWA UNIVERSITY OF TECHNOLOGY, 19 ARMII KRAJOWEJ AV, 42-200 CZĘSTOCHOWA, POLAND
*** MEDICAL UNIVERSITY OF SILESIA, 3 KASZTANOWA STR., 41-200 SOSNOWIEC, POLAND

Corresponding author: kulesza@matman.uwm.edu.pl

182

2. Experimental

Free edge of healthy nail was acquired from 18-years-old female and cut into a series of small, rectangular pieces firmly attached to AFM sample discs. The discs were then transferred to a Petri dish and covered with a droplet of acetone such that the nails were completely immersed in the liquid. The Petri dish was closed and the nails were incubated for 2 and 4 min. at room temperature. After that, the samples were dried, scanned using Atomic Force Microscopy (AFM) and left for aging. The samples were exposed for 2 years to ambient air under the following conditions: sub-room temperature 18°C, atmospheric pressure (might slightly vary), relative humidity 50%. Changes in surface geometry of the nails were studied using both AFM and SEM. AFM measurements were carried out using Multimode 8 (Bruker) instrument and the Scanasyst-Air probe (Bruker) working in the tapping mode. The instrument enables direct tip-surface force control (PeakForce Tapping) and maps nanomechanical properties of the scanned surface, including Young's modulus (Quantitative Nanomechanical Mapping). The probe was made of SiN with triangular cantilever and the following parameters: nominal resonant frequency 70 kHz, spring constant 0.4 N/m, tip radius 2 nm. Maximum press force achieved in a PeakForce tapping mode was kept at 1 nN.

3. Theory

Euclidean geometry deals with objects with well-developed habits and integer dimensions. Apart from that, however, there are also irregular and discontinuous structures that behave as if they have non-integer dimensions. Their main feature include (limited) geometrical self-similarity, that is the scale-invariance. Previous works on surface engineering of materials demonstrated that popular statistical parameters based on data distribution functions (e.g. mean height, standard deviation, higher moments etc.) of height data do not provide any unique specification of rough surfaces [16-18], and that more accurate characteristics of spatial complexity can be brought by fractal analysis [19-22]. Regardless of the acquisition method, fractal descriptors can be derived by making use of allometric scaling among data samples,

which was described in details elsewhere [23-27]. An outline of the routine includes calculation of such parameters as: anisotropy ratio S_{tr}, corner frequency τ, fractal dimension D etc., via auto-correlation and height-height correlation (structure) functions.

4. Results and discussion

4.1. As-cut nails exposed to acetone

Fig. 1 presents 50×50 μm^2 AFM images of the as-cut nails before and after exposure to acetone. Topography images exhibit flat nail plates crossed with irregular trenches, although visual appearance does not reveal significant differences between scanned sections. Fortunately, structural changes are reflected in spatial characteristics presented in Table 1. First of all, untreated sample is found monofractal with only one fractal dimension D equal to 2.41. The surface is also isotropic, since anisotropy ratio S_{tr} approaches 0.79. However, the above scaling behavior vanishes within a distance set by the corner frequency, which is one order of magnitude smaller than the scan length. In contrast, samples exposed to acetone are found bifractal with a second-order alignment pattern of geometrical objects of dimensions less than 2 nm in size. Split in fractal characteristics might be due to chemical-stimulated abrasion of the nail surface that unveils deeper lying structures.

TABLE 1

Surface texture characteristics of nails exposed to acetone derived from AFM images (50×50 μm^2): S_q – RMS surface roughness, S_{dr} – developed interfacial area ratio, S_{tr} – surface anisotropy ratio, Y_{AV} – average Young's Modulus, D – fractal dimension, and τ – corner frequency

Sample	S_q [nm]	S_{dr} [%]	S_{tr}	Y_{AV} [MPa]	D_1	τ_1 [mm]	D_2	τ_2 [mm]
Ref.	320	6.3	0.79	2000	—	—	2.41	5.10
2 min.	450	9.0	0.91	1900	2.41	1.97	2.66	8.43
4 min.	240	4.3	0.55	760	2.42	1.92	2.72	7.78

Apart from qualitative changes in fractality, obtained statistical parameters, namely: interfacial area ratio S_{dr}, anisotropy ra-

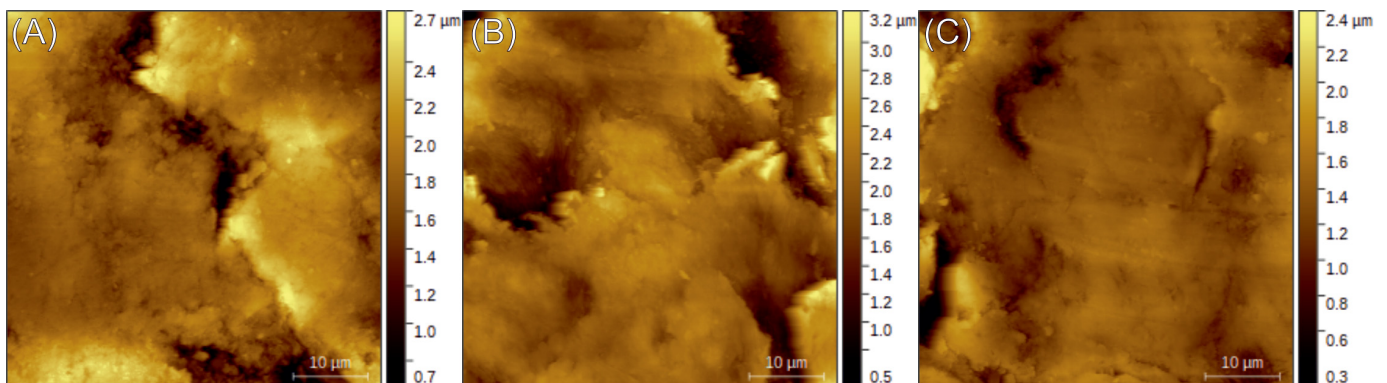

Fig. 1. AFM images of the as-cut nails exposed to acetone (50×50 μm^2): (A) reference sample, (B) 2 min exposure, (C) 4 min exposure

tio S_{tr} and Young's modulus might suggest further changes in the surface development and its elastic properties at the nanoscale. In the beginning of the exposure routine the nails become more isotropic and more developed, but then the process turns downwards, and the surface becomes more compact and more anisotropic. On the other hand, elastic modulus Y_{AV} steadily decreases from 2000 down to 760 MPa with increasing exposure time. To conclude the above results, the plate under study is the hard part of the nail, made of translucent keratin protein. Several layers of dead, compacted cells cause the nail to be strong but flexible, however, due to the dehydrating aspects of acetone, super dry, damaged nails will get more brittle. Further exposure to this liquid might eventually lead to splitting, peeling and breakage, because the solvent will bathe the uppermost parts of the plate.

4.2. Aged nails

Fig. 2 shows AFM images of the same nails as in Fig. 1, although subject to prolonged aging under atmospheric conditions. Similar to previous results, there is no difference between samples in their visual appearance. In fact, significant changes can be seen considering fractal and statistical characteristics summarized in Table 2.

TABLE 2

Surface texture characteristics of nails exposed to acetone and subsequently routinely stored under atmospheric conditions, derived from AFM images (50×50 μm²): S_q – RMS surface r oughness, S_{dr} – developed interfacial area ratio, S_{tr} – surface anisotropy ratio, Y_{AV} – average Young's Modulus, D – fractal dimension, and τ – corner frequency

Sample	S_q [nm]	S_{dr} [%]	S_{tr}	Y_{AV} [MPa]	D_1	τ_1 [mm]	D_2	τ_2 [mm]
Ref.	260	3.8	0.69	1700	2.48	1.56	2.55	7.25
2 min.	270	4.3	0.52	7100	2.45	1.26	2.54	6.89
4 min.	330	5.3	0.30	3200	2.37	1.08	2.49	6.30

All samples exhibit bifractal characteristics, which means that the nails tend to re-arrange their surface structure under the influence of chemical solvents. In addition, the plates maintain their cluster sub-structure, in which smaller components (~1 μm) aggregate into larger structures (7 μm in diameter). What is more interesting, the fractal dimension D_1 is close to that in as-cut samples, while the lower corner frequency τ_1 is smaller by the factor of three. Likewise, the fractal dimension D_2 remains constant at around 2.5 throughout the series, but appears smaller compared with as-cut specimens.

Statistical parameters reveal compact, dense-packed surface with anisotropic spatial alignment of various degree. Interestingly, elastic modulus Y_{AV} in the reference sample is found close to that in as-cut, exposed for 2 min to acetone. On the other hand, the sample that was aged after 2 min treatment with acetone turns out to have the highest elastic modulus approaching 7100 MPa, i.e. over four times higher than the reference sample. Even the sample treated for 4 min exhibits substantially raised elastic modulus (3200 MPa), which might be possibly attributed to the sorption of water vapors.

Fig. 3 presents SEM images of the nails taken with 1000× magnification. Because of similar dimensions, it might be interesting to compare spatial characteristics derived from SEM images to those obtained by AFM. At a glance, SEM images of the specimen do not differ significantly upon performed treatment. Unlike topographical appearance, however, fractal characteristics reveal bifractal nature of the specimens. Note that fractal dimension D_1 derived from SEM is larger than that from AFM, but D_2 is very similar. As a result, the trend in the structure functions is bent downwards, unlike previous measurements. Apart from that, corner frequency τ_1 is smaller by a factor of two, while τ_2 two

TABLE 3

Surface texture characteristics of nails exposed to acetone and routinely stored under atmospheric conditions, derived from SEM images taken with 1000× magnification: S_q – RMS surface roughness, S_{tr} – surface anisotropy ratio, D – fractal dimension, and τ – corner frequency

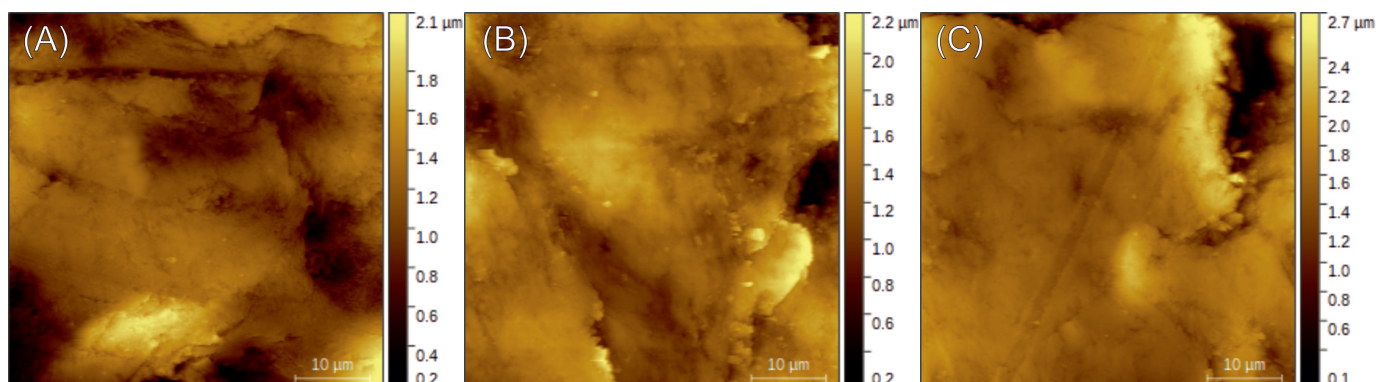| Sample	S_{tr}	D_1	τ_1 [mm]	D_2	τ_2 [mm]
Ref	0.96	2.71	0.86	2.56	15.3
2 min.	0.71	2.57	0.42	2.44	14.5
4 min.	0.32	2.53	0.62	2.42	10.5

Fig. 2. AFM images of the aged nails previously exposed to acetone (50×50 μm²): (A) reference sample, (B) 2 min exposure, (C) 4 min exposure

184
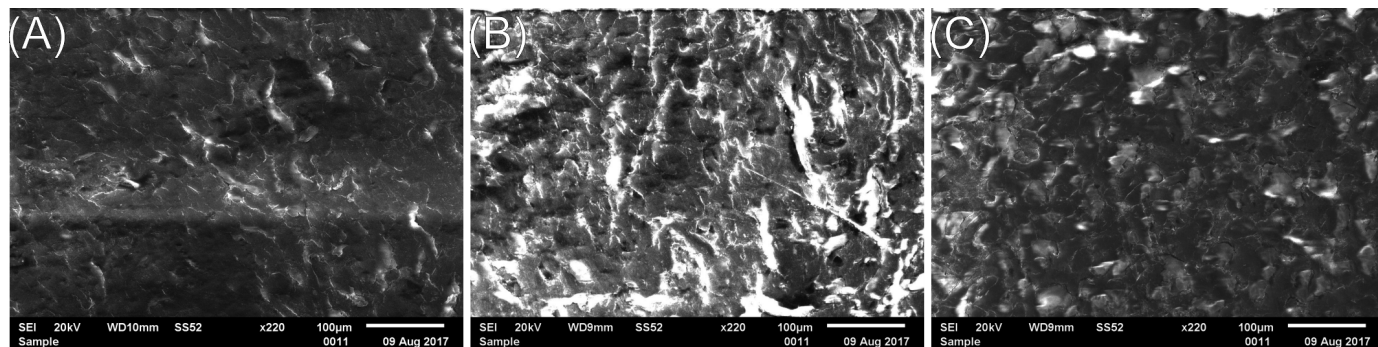

Fig. 3. SEM images of the aged nails previously exposed to acetone, taken at 1000× magnification (128×87 μm^2): (A) reference sample, (B) 2 min exposure, (C) 4 min exposure

times larger than those in the as-cut samples. Observed discrepancies in the corner frequency values might be due to improper linearization procedure that converted grayscale SEM images into pseudo-height maps using direct proportionality routine.

5. Conclusions

As-cut fingernails exhibit monofractal characteristics, although their scaling behavior breaks down at distances of one order of magnitude smaller than the scan length. Human nails are found to undergo structural reconstruction under chemical treatment from monofractal into bifractal geometry, which means that higher-order surface patterns appear. The appearance of long-range surface patterns is independent of the chemical treatment: agressive factor (acetone) as well as mild ones (atmospheric oxygen) exert similar influence. Acetone affects the sample geometry in a twofold way: initially enhances surface development, but then makes the surface more compact. Apart from that, acetone lowers the elastic modulus of the plates. In turn, aging diminishes variations in the surface height amplitude but preserves trends in surface geometry measures. On the other hand, texture anisotropy steadily decreases to very low values. Regardless of the imaging method, fractal characteristics of the samples under study are similar.

REFERENCES

[1] M.K. Shin, K.S. Kim, J.J. Ahn, Clin. Exp. Dermatol. **37** (2), 156-63 (2012).

[2] C. LaTorre, B. Bhushan, Ultramicrosc. **105**, 155-175 (2005).

[3] J. Liu, P. Lei, J. Am. Acad. Dermatol. **49** (2 Suppl Case Reports), S154-6 (2003).

[4] M.M. Jiaravuthisan, D. Sasseville, R.B. Vender, J. Am. Acad. Dermatol. **57**, 1-27 (2007).

[5] S.P. Gurden, V.F. Monteiro, E. Longo, J. Microsc. **215**, 13-23 (2004).

[6] S. Murdan, C. Poojary, D.R. Patel, Int. J. Cosmet. Sci. **34** (3), 257-62 (2012).

[7] S. Murdan, Expert Opin. Drug Deliv. **5** (11), 1267-82 (2008).

[8] B. Werner, A. Antunes, Dermatol. Pract. Concept. **3** (3), 9-14 (2013).

[9] M. Miteva, D.C. de Farias, Arch. Dermatol. **147** (9), 1117-8 (2011).

[10] O. Barak, A. Asarch, T. Horn, J. Cutan. Pathol. **37** (10), 1038-40 (2010).

[11] D. Wilsmann-Theis, F. Sareika, T. Bieber, J. Eur. Acad. Dermatol. Venereol. **25** (2), 235-7 (2011).

[12] N.W. Coleman, P. Fleckman, J.I. Huang, J. Hand. Surg. Am. **39** (5), 985-8 (2014).

[13] X. Yue, Q. Li, H. Wang, Y. Sun, Scanning **38** (2), 172-6 (2016).

[14] C. Plozzer, C. Coletti, F. Kokelj. Acta Derm. Venerol. Suppl. **211**, 9-11 (2000).

[15] S.R. Vaka, S.N. Murthy, J.H. O'Haver, M.A. Repka, Drug. Dev. Ind. Pharm. **37** (1), 72-79 (2011).

[16] M. Zare, S. Solaymani, A. Shafiekhani, S. Kulesza, Ş. Ţălu, M. Bramowicz, Sci. Rep. **8**, 10870 (2018).

[17] S. Solaymani, A. Ghaderi, L. Dejam, Z. Garczyk, W. Sapota, S. Stach, V. Dalouji, C. Luna, S.M. Elahia, S.H. Elahi, Int. J. Hyd. En. **42** (20), 14205-14219 (2017).

[18] S. Solaymani, S. Kulesza, S. Talu, M. Bramowicz, N.N. Beryani, V. Dalouji, S. Rezaee, H. Karami, M. Malekzaden, E.S. Dorbidi, J. Alloys Comp. **765**, 180-185 (2018).

[19] Ş. Ţălu, S. Solaymani, M. Bramowicz, J. Mater. Sci.: Mater. Electron. **27** (9), 9272-9277 (2016).

[20] N. Naseri, S. Solaymani, A. Ghaderi, RSC Adv. **7**, 12923-12930 (2017).

[21] M. Bramowicz, S. Kulesza, T. Lipiński, Sol. State Phen. **203-204**, 86-89 (2013).

[22] M. Bramowicz, S. Kulesza, P. Czaja, W. Maziarz, Arch. Metal. Mater. **59**, 451-457 (2014).

[23] Ş. Ţălu, M. Bramowicz, S. Kulesza, J. Ind. Eng. Chem. **35**, 158-166 (2016).

[24] S. Kulesza, M. Bramowicz, Appl. Surf. Sci. **293**, 196-201 (2014).

[25] Ş. Ţălu, M. Bramowicz, S. Kulesza, V. Dalouji, S. Solaymani, S. Valedbagi, Microsc. Res. Tech. **79**, 1208-1213 (2016).

[26] N. Papež, D. Sobola, L. Škvarenina, P. Škarvada, D. Hemzal, P. Tofela, L. Grmela, Appl. Surf. Sci. **461**, 212-220 (2018).

[27] D. Sobola, S. Talu, P. Sadovsky, N. Papez, L. Grmela, Adv. Electric. Electron. Eng. **15**, 569-576 (2017).